Oriented crystallization of calcite single crystals grown underneath monolayers of tetracarboxyresorc[4]arenes

Dirk Volkmer, Marc Fricke, Ceno Agena, Jochen Mattay

Angaben zur Veröffentlichung / Publication details:

Volkmer, Dirk, Marc Fricke, Ceno Agena, and Jochen Mattay. 2002. "Oriented crystallization of calcite single crystals grown underneath monolayers of tetracarboxyresorc[4]arenes." *CrystEngComm* 4 (52): 288–95. https://doi.org/10.1039/b202208g.

Oriented crystallization of calcite single crystals grown underneath monolayers of tetracarboxyresorc[4]arenes†

Dirk Volkmer,*[a] Marc Fricke,[a] Ceno Agena[b] and Jochen Mattay[b]

[a] *University of Bielefeld, Faculty of Chemistry (AC1), Bielefeld, Germany. E-mail: dirk.volkmer@uni-bielefeld.de*
[b] *University of Bielefeld, Faculty of Chemistry (OC1), Bielefeld, Germany. E-mail: mattay@uni-bielefeld.de*

The crystal structures of *rccc*-5,11,17,23-tetracarboxy-4,6,10,12,16,18,22,24-octa-*O*-methyl-2,8,14,20-tetra(*n*-undecyl)resorc[4]arene, **1**, and its Ca salt, **2**, are described. Structural data were analyzed in terms of supramolecular packing motifs of the constituent amphiphilic macrocycles. Monolayer experiments indicate that a similar packing arrangement can be predicted for monolayers of **1** spread at the air–water interface. $CaCO_3$ (calcite) single crystals were grown underneath monolayers of **1** with highly uniform (012) orientation. This particular orientation was observed for a variety of structurally dissimilar monolayers indicating that macroscopic film properties such as average charge density or mean dipole moment have a decisive influence on templated calcite growth.

Introduction

Much attention has been devoted to the characterization of mineral phases which occur in biominerals and calcified tissues.[1] Among the many open questions, one of the most challenging scientific problems is to gain insights into the molecular interactions that occur at the interface between the inorganic mineral and the macromolecular organic matrix. For the most widespread calcified tissues it is frequently assumed that a structurally rigid composite matrix consisting of fibrous proteins and thereon adsorbed acidic macromolecules acts as a supramolecular "blueprint" that templates nucleation of the inorganic phase.[2]

Efforts in trying to separate and mimic aspects of these complex interactions with simple model systems will help to improve our understanding of crystallization processes that are under biological control. However, the deliberate design of interface architectures that direct crystal nucleation and growth in a predictable manner is by and large still a matter of trial and error.

Chemists have employed different experimental set-ups to create highly-ordered template surfaces, including Langmuir monolayers,[3] self-assembled monolayers (SAMs),[4] or thin films.[5] Especially the crystallization of inorganic compounds underneath free floating monolayers of amphiphilic molecules bears much development potential, since the surface properties may be adjusted by a suitable surfactant design as well as by simple experimental control parameters (*i.e.* subphase composition, surface area/molecule, or temperature).

We have recently initiated a research project focussing on induced crystallization underneath Langmuir monolayers of amphiphilic oligoacids.[6] We here describe crystal structure analysis of *rccc*-5,11,17,23-tetracarboxy-4,6,10,12,16,18,22,24-octa-*O*-methyl-2,8,14,20-tetra(*n*-undecyl)resorc[4]arene, **1**, a novel surfactant bearing carboxy substituents at the resorcinol 2-positions (Scheme 1b), and its Ca salt, **2**.

Resorcinol-derived metacyclophanes have been subject of intense research since their original preparation in 1872.[7] The first X-ray structural characterization of a resorc[4]arene was reported in 1968.[8] Since then, resorcarene supramolecular architectures have been developed largely by the pioneering work of Cram *et al.*[9] using conformationally immobile resorcarenes (cavitands,[10] carcerands[11]) which show a rich and fascinating host–guest chemistry.

In contrast to numerous studies dealing with their complexation properties in solution,[12] resorcarenes have rarely been used for the construction of infinite 2-dimensional architectures (*i.e.* monolayers, thin films)[13] or 3-dimensional solids.[14] This is surprising in light of certain molecular topological features that should render this class of macrocycles particularly attractive for crystal engineering purposes: resorcarenes bearing various substituents (*e.g.* H, OH, Me) at the resorcinol 2-position are readily synthesized in gram quantities through one-pot acid catalyzed condensation with

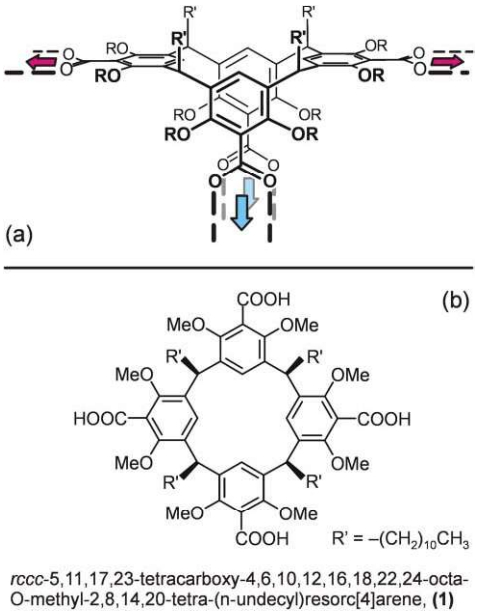

rccc-5,11,17,23-tetracarboxy-4,6,10,12,16,18,22,24-octa-O-methyl-2,8,14,20-tetra-(n-undecyl)resorc[4]arene, **(1)**

Scheme 1

†Based on the presentation given at CrystEngComm Discussion, 29th June–1st July 2002, Bristol, UK.

aldehydes. Generally, the all-*cis* configured (*rccc*), bowl-shaped cyclic tetramer is precipitated in the course of the reaction because of its low solubility in acidic aqueous media. Under kinetic control of reaction conditions, the *cis–trans–trans* isomer (*rctt*) can also be isolated. According to X-ray structure analysis, *rccc*-resorcarenes with free hydroxy groups often yield structures in the bowl-shaped C_{4v}-symmetric *crown* conformation,[15] whereas resorcarene derivatives containing (non-bridging) *O*-alkyl substituents yield structures in the *boat* conformation.

Of special interest here is the less common C_{2v}-symmetric boat conformer where two benzene rings face each other, whereas the other ones lie in a common plane (Scheme 1a). This particular conformation results in a rectangular arrangement of functional groups (which represents a rare case for neat organic structures).

We furthermore describe our first results on induced crystallization of calcium carbonate underneath monolayers of **1**. Monolayers are spread on aqueous subphases of various compositions and the corresponding Langmuir isotherms are analyzed in terms of possible supramolecular packing arrangements. The occurrence of uniformly oriented calcite ($CaCO_3$) single crystals is monitored *in situ* by (polarization) optical microscopy. The orientation of epitaxially grown calcite crystals with respect to the monolayer is determined by means of X-ray diffraction, scanning electron microscopy and optical microscopy.

Results

X-Ray crystallographic investigations

Structure analysis of resorcarenes in boat conformations have so far been achieved quite a few times. A search of the Cambridge Structural Database (February 2002) yielded a subtotal of 14 X-ray structures out of 121 resorcarenes structures in all. No structures of *rccc*-resorcarenes with boat conformations containing *n*-undecyl residues have been obtained so far. The X-ray crystallographic investigations on single crystals of *rccc*-5,11,17,23-tetracarboxy-4,6,10,12,16,18,22,24-octa-*O*-methyl-2,8,14,20-tetra(*n*-undecyl)resorc[4]arene, **1**, and its Ca salt, **2**, presented here (Table 1) are the first structural examples of a metal-free resorc[4]arene acid and its corresponding Ca complex.

Crystal structure of 1

Single crystals of the compound $C_{84}H_{128}O_{16}\cdot(CH_3CN)_{1/8}$, **1**, were obtained by slow recrystallization from acetonitrile solution kept at 60 °C.

Important features of the resorcarene's molecular geometry are described by a few geometrical parameters as defined in Scheme 2.

The asymmetric unit of **1** contains two molecules which differ mainly by the arrangement of resorcarene methoxy substituents.

The X-ray structure analysis shows that compound **1** adopts a highly symmetrical boat conformation. which is described by the folding angle φ between least squares planes running through atomic positions of opposite benzene rings. For the first resorcarene molecule, φ_1 is 167.5°, while φ_2 amounts to 3.5°; the center-to-center spacing d between opposite benzene rings is 4.96 Å. While two out of four undecyl chains adopt an energetically favorable all-*trans* conformation (the largest deviation from the ideal torsion angle, $\theta = 180°$, being 11°), the other ones display a single *gauche* "defect" (av. $\theta = 70.7°$) occurring at atomic positions 1, 2, 3, and 4 of the undecyl chains. The corresponding values for the second molecule of the asymmetric unit are very similar ($\varphi_1 = 169.0°$; $\varphi_2 = 6.9°$; $d = 4.90$ Å; av. $\theta = 61.0°$).

Compound **1** forms a lamellar structure where the hydrophilic constituents (carboxylic acid residues) and the hydrophobic residues (undecyl chains) segregate into different layers. The boat conformation of the macrocycles gives rise to formation of infinite, 2-dimensional flat strands consisting of resorcarene molecules which are interconnected through

Table 1 X-Ray crystallographic data for compounds **1** and **2**[a]

Compound	**1**	**2**
Formula	$C_{84}H_{128}O_{16}\cdot(CH_3CN)_{1/8}$	$[Ca(C_{84}H_{126}O_{16})(DMSO)_2(H_2O)_2]\cdot DMSO\cdot(H_2O)_4$
M_r/g mol^{-1}	1399.00	1774.41
T/K	183(2)	183(2)
λ/Å	0.71073	0.71073
Crystal system	monoclinic	triclinic
Space group	$P2_{(1)}/m$	$P\bar{1}$
a/Å	17.5950(8)	13.1315(8)
b/Å	58.099(3)	14.2389(8)
c/Å	18.2362(9)	28.243(2)
α/°	90	78.618(1)
β/°	93.977(1)	86.426(1)
γ/°	90	78.260(1)
V/Å^3	18597.0(15)	5067.3(5)
Z	8	2
ρ_{calcd}/g cm^{-3}	0.999	1.163
μ(Mo-K$_\alpha$)/mm^{-1}	0.068	0.191
F(000)	6102	1928
Crystal size/mm	0.10 × 0.25 × 0.40	0.02 × 0.40 × 0.50
θ range/°	1.12–22.52	1.47–25.01
Index ranges	$-18 \leqslant h \leqslant 18$, $-55 \leqslant k \leqslant 62$, $-19 \leqslant l \leqslant 16$	$-15 \leqslant h \leqslant 15$, $-16 \leqslant k \leqslant 16$, $-33 \leqslant l \leqslant 33$
Reflections collected	76378	45705
R(int)	0.0425	0.0488
Independent reflections	24569	17813
Data/restraints/parameters	24569/0/1848	17813/0/1089
GoF	1.057	0.986
R values [$I > 2\sigma(I)$][b]	$R_1 = 0.0950$, $wR_2 = 0.2884$	$R_1 = 0.0707$, $wR_2 = 0.2005$
R values (all data)[b]	$R_1 = 0.1319$, $wR_2 = 0.3176$	$R_1 = 0.1149$, $wR_2 = 0.2211$
Weighting scheme, w^{-1}[c]	$[\sigma^2(F_o^2) + (0.1653\cdot P)^2 + 48.1\cdot P]$	$[\sigma^2(F_o^2) + (0.1387\cdot P)^2 + 0.00\cdot P]$
Largest diff. peak/hole/e Å^{-3}	1.015/−0.384	1.179/−0.517

[a]Click here for full crystallographic data (CCDC 183961 and 183962). [b]$R_1 = \Sigma||F_o| - |F_c||/\Sigma|F_o|$; $wR_2 = [\Sigma w(F_o^2 - F_c^2)^2/\Sigma w(F_o^2)^2]^{1/2}$. [c]$P = (F_o^2 + 2\cdot F_c^2)/3$.

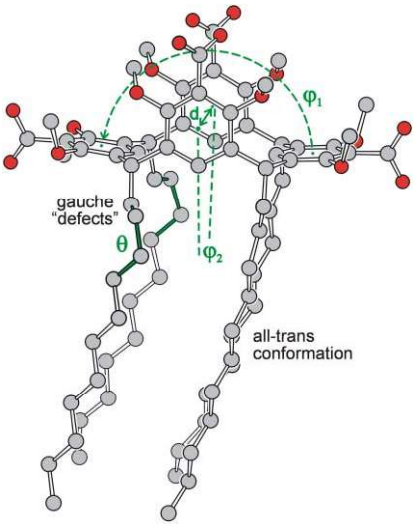

Scheme 2 Definition of geometrical parameters used to describe the molecular structure of resorcarene moieties in the crystal structures of **1** and **2**. $\varphi_{1,2}$: folding angles between least squares planes running through atomic positions of opposite benzene rings; *d*: center-to-center spacing of opposite benzene rings; θ: torsion angle describing *gauche* "defects" occurring at selected atomic positions of the undecyl chains.

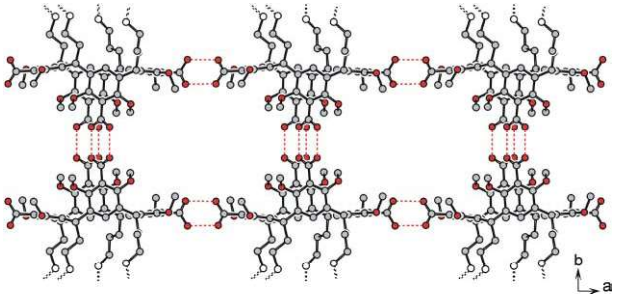

Fig. 1 Ball-and-stick model of the hydrogen bonding scheme in the crystal lattice of **1**. (Hydrogen atoms and fractions of the *n*-undecyl chains are omitted for clarity.)

hydrogen bonds between carboxylic acid residues (Fig. 1). These strands form layers in the crystallographic *ac*-plane. The average surface area occupied by a single resorcarene molecule

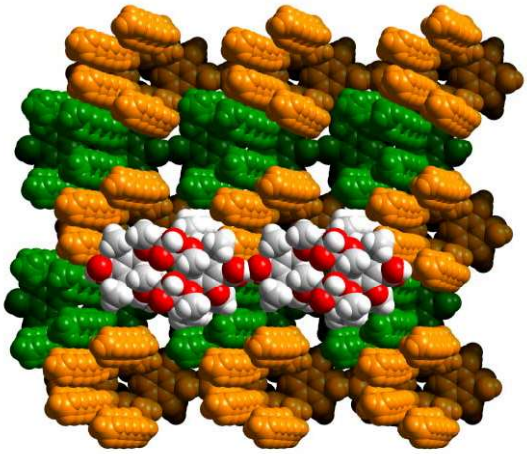

Fig. 2 Space-filling model of the supramolecular packing arrangement of **1** in the crystal lattice.

in the *ac*-plane amounts to 160 $Å^2$. The resulting packing arrangement is reminiscent of an "inverted" bilayer structure motif (Fig. 2), which is dictated by a close packing of hydrophilic head groups (as opposed to the close packing of hydrophobic alkyl chains in the bilayer structure of common surfactants or lipids).

Fig. 2 shows a space filling model of the supramolecular packing arrangement of **1** in the crystal lattice. Different strands of interconnected resorcarene molecules are highlighted in orange and green, respectively. The undecyl chains are tilted by an average angle of 20° against the *ac*-plane normal. Since the undecyl chains of an isolated bilayer are not bulky enough to fill the space completely (Fig. 2), interdigitation of successive bilayers occurs while bilayer stacking follows the *b*-direction (Fig. 3). The occurrence of *gauche* "defects" in the conformation of half of the undecyl chains may represent a further adaptation of the molecules to avoid empty spaces.

Crystal structure of 2

Single crystals of compound $[Ca(C_{84}H_{126}O_{16})(DMSO)_2(H_2O)_2]\cdot DMSO\cdot(H_2O)_4$, **2**, were obtained at room temperature by slow vapor diffusion of water into a DMSO solution of **2**.

The asymmetric unit of **2** contains one half of a dinuclear Ca

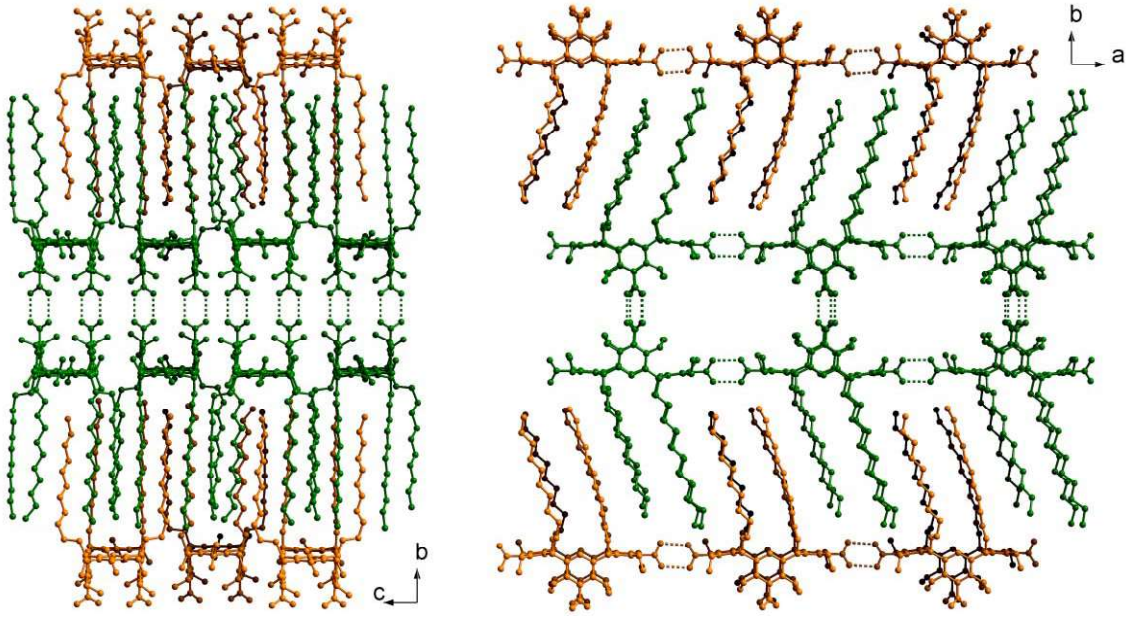

Fig. 3 Packing diagrams showing the interdigitation of bilayers of **1** in the crystal lattice. Resorcarene molecules belonging to the same "inverted" bilayer are represented with identical colors (hydrogen atoms are omitted for clarity). Click image or here to access a 3D representation.

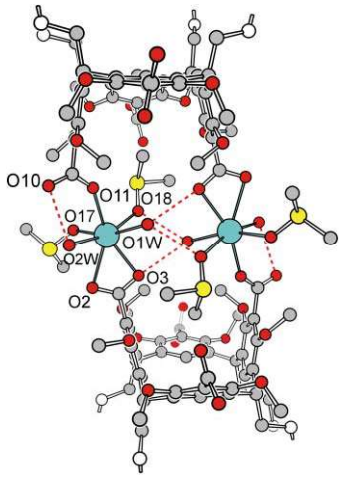

Fig. 4 Coordination scheme of the dinuclear Ca complex, **2**. Intramolecular hydrogen bonds between different oxygen donor ligands are displayed as broken red lines. (Hydrogen atoms and fractions of the *n*-undecyl chains are omitted for clarity.)

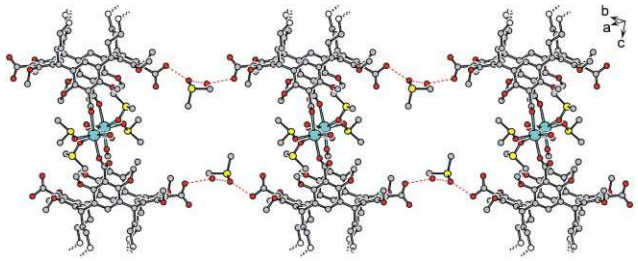

Fig. 5 Ball-and-stick model of the intermolecular hydrogen bonding scheme in the crystal lattice of **2**. (Hydrogen atoms and fractions of the *n*-undecyl chains are omitted for clarity.)

complex which is described by the molecular formula $[Ca(C_{84}H_{126}O_{16})(DMSO)_2(H_2O)_2]_2$. The coordination scheme of Ca ions is shown in Fig. 4. Each Ca ion is placed in a distorted pentagonal bipyramidal coordination environment consisting of different oxygen donor ligands (two DMSO molecules, two water molecules, and two carboxylate residues belonging to different resorcarene moieties, respectively). The carboxylate residues show different coordination modes, one

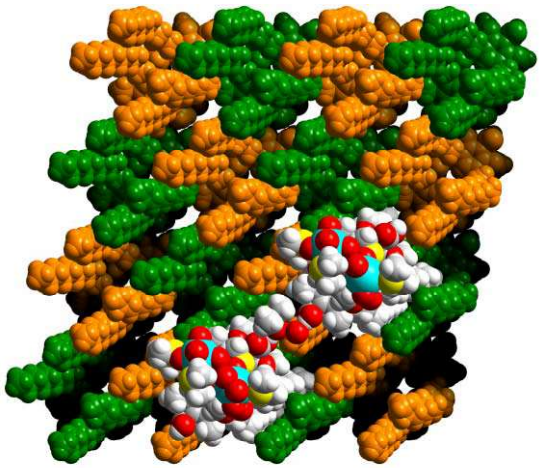

Fig. 6 Space-filling model of the supramolecular packing arrangement of **2** in the crystal lattice.

residue is coordinated in a monodentate fashion whereas the other one is coordinated in the bidentate (η^2) mode to the Ca ion. The oxygen donor ligands of the dinuclear unit are extensively interconnected by means of intra- and intermolecular hydrogen bonds which are shown in Fig. 4 and 5.

The gross structural features of the free acid **1** are likewise observed in the crystal structure of its corresponding Ca complex, **2**. Compound **2** also forms a lamellar structure where the hydrophilic constituents (carboxylate residues, oxygen donor ligands) and the hydrophobic residues (undecyl chains) segregate into different layers (Fig. 6 and 7).

The boat conformation of the macrocycles gives rise to formation of infinite, 2-dimensional flat strands consisting of the dinuclear units which are interconnected through hydrogen bonds. The *inter*molecular hydrogen bonding scheme, however, is dissimilar to that of the free acid. As shown in Fig. 5, the hydrogen bonds between non-coordinated carboxylic acid residues are intercepted by a single DMSO and a water molecule, respectively, which leads to a less dense packing of resorcarene ligands. The average surface area occupied by a single resorcarene molecule in the *ab*-plane therefore amounts to 183 $Å^2$.

X-Ray structure analysis shows that the resorcarene molecules in the crystal structure of **2** adopt a boat

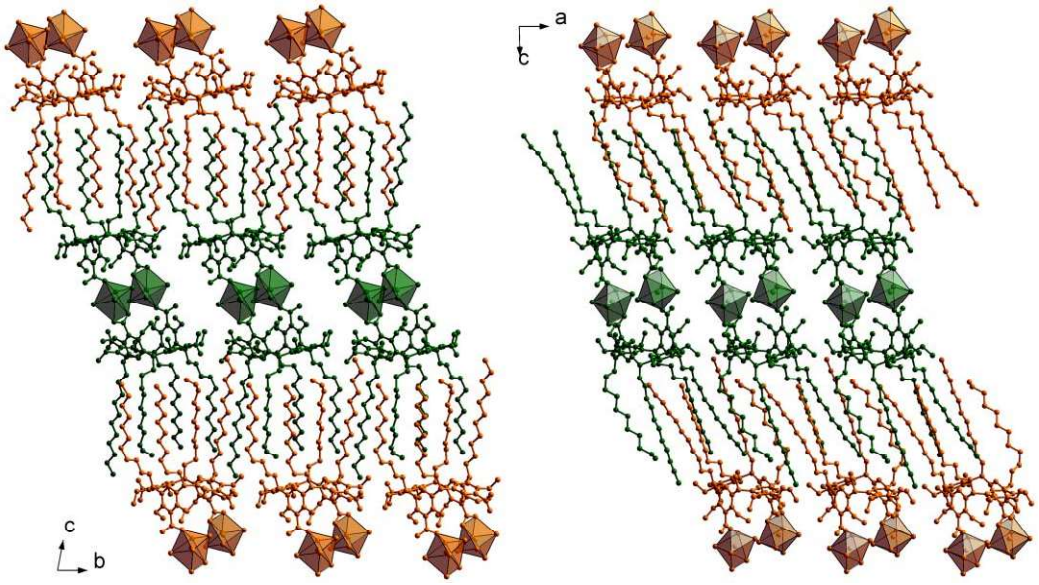

Fig. 7 Packing diagrams showing the interdigitation of bilayers of **2** in the crystal lattice. Resorcarene molecules belonging to the same "inverted" bilayer are represented with identical colors (hydrogen atoms are omitted for clarity; only the oxygen donor atoms of the Ca coordination environment are shown). Click image or here to access a 3D representation.

conformation which is distorted from ideal rectangular geometry as defined in Scheme 1a. The folding angle φ_1 is 146.4°, while φ_2 amounts to 22.4°; the center-to-center spacing d between opposite benzene rings is 5.52 Å. Only one of four undecyl chains adopts an energetically favorable all-*trans* conformation (the largest deviation from the ideal torsion angle $\theta = 180°$ being 15°), the other ones display a single *gauche* "defect" (av. $\theta = 67.5°$) occurring at atomic positions 1, 2, 3, and 4 of the undecyl chains. One of these chains shows a second *gauche* "defect" ($\theta = 88°$) occurring at atomic positions 8, 9, 10, and 11.

An important question arises as to whether or not the (almost) rectangular geometry of resorcarene boat conformers in the crystal structure of **1** represents a favourable situation in terms of steric energy. In principal, it is conceivable that the gain of energy through formation of hydrogen-bonded oligomers in the structure of **2** leads to over-compensation of any steric strain which is imposed upon the macrocyclic backbone as it approaches a rectangular arrangement. Breaking the hydrogen bonds by means of solvent insertion, as observed in the crystal structure of **2**, may then lead to a more relaxed resorcarene geometry.

A close inspection of published resorcarene structural data, however, shows that in fact the rectangular arrangement seems to be favorable, at least in terms of crystal packing energy. The Cambridge Structural Database contains structural data of resorcarene derivatives 4,6,10,12,16,18,22,24-octa-*O*-methyl-2,8,14,20-tetra(isopropoxycarbonylmethyl)resorc[4]arene ($C_{56}H_{72}O_{16}$, CSD structure code: HEFKUY10),[16] and of 4,6,10,12,16,18,22,24-octa-*O*-ethyl-2,8,14,20-tetramethylresorc-[4]arene ($C_{48}H_{64}O_8$, CSD structure code: POBCUE).[17] Both derivatives show an almost perfect rectangular boat conformation, although they do not contain any acidic substituents that are capable of forming hydrogen bonds.

Monolayer studies

Crystallographic investigations on the solid state structure of the amphiphilic resorcarene **1**, and its Ca salt, **2**, are complemented by monolayer studies.

Langmuir monolayers

An advantage of the monolayer technique using a film balance is that characteristic features of the monolayer, *e.g.* surface pressure, macroscopic texture and lattice structure, can be studied as a function of area per molecule. The surface pressure (π)–area (A) isotherms provide information on the thermodynamics and the phase behaviour of the monolayer.

Fig. 8 shows the π–A isotherms of compound **1** monolayers spread on an aqueous subphase (pure water, and 10 mM $CaCl_2$, respectively). In both cases, stable monolayers are formed which collapse upon compression at a surface pressure of ~40 mN m^{-1}.

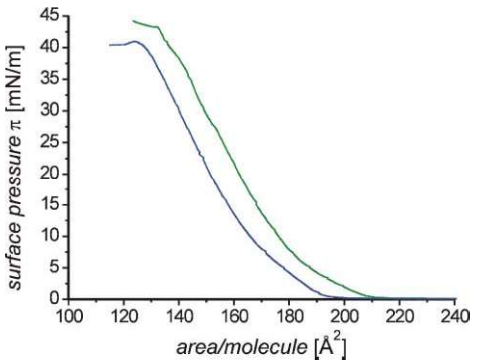

Fig. 8 π–A isotherms of monolayers of **1** at 24 °C on H_2O (blue), and aqueous 10 mM $CaCl_2$ (green).

Table 2 Area per molecule of 2,8,14,20-tetra(*n*-undecyl)resorc[4]arene derivatives as determined from crystal data and Langmuir isotherms

Compound	Area per molecule/Å^2	Ref.
1	160;[a] 170[b] (H_2O)	This work
2	183;[a] 180[b] (10 mM $CaCl_2$)	This work
$C_{72}H_{112}O_8 \cdot 4EtOH$	158;[a] 170[b] (H_2O)	19[c]

[a]Crystal structure data. [b]Monolayer data (subphase composition). [c]Data estimated from Langmuir isotherms as displayed in the article.

Upon addition of $CaCl_2$, the Langmuir isotherm displays a parallel shift toward higher area-per-molecule values. The constant shape of the isotherms indicates a similar phase behaviour for both subphase compositions. The straight pressure increase over a comparatively large region of the molecular area suggests fluid properties of the condensed phase. On a pure aqueous subphase the pressure increase starts at ~195 Å^2 molecule^{-1} and on 10 mM $CaCl_2$ solution at ~210 Å^2 molecule^{-1}.

The area per molecule of **1** in the monolayers is estimated from extrapolating the Langmuir isotherms toward zero pressure. The determined area values are listed in Table 2. In both cases, monolayer data are in excellent agreement with the surface area per molecule as determined from crystal structure analysis. On a subphase containing 10 mM $CaCl_2$, the molecular area of **1** shows a significant increase as compared to corresponding value of the monolayer if spread on pure water. We assume that this behaviour is due to electrostatic/coordinative interactions of Ca ions which cause the carboxylic acid residues of **1** to become deprotonated. Expansion effects of monolayers spread on metal ion-containing subphases, similar to those observed here, have been reported for several systems.[18]

The monolayer data obtained so far strongly indicate that the packing arrangements of molecules in the monolayer and in the crystal lattice are similar. The two-dimensional packing of the condensed monolayer phase is obviously determined by the bulky polar head group and not by the alkyl chains (for the latter case, much more complicated monolayer phase behavior should be observed).

A more refined examination of the monolayer phase diagram of **1**, including Brewster-angle microscopic investigations of film texture as a function of pH and subphase composition, is currently underway and will be presented elsewhere.[20]

$CaCO_3$ crystallization underneath monolayers

Crystallization of calcium carbonate underneath monolayers of **1** leads to formation of uniformly oriented calcite single crystals at low compression (π = 0.1–0.5 mN m^{-1}), while more randomly oriented single crystals are obtained at higher surface pressure (π = 5–20 mN m^{-1}). Crystal growth is observed *in situ* by polarization (optical) microscopy (Fig. 9).

In order to determine the orientation of calcite crystals relative to the monolayer, X-ray powder diffraction (XRD) measurements were performed in reflection mode on polycrystalline film patches that were transferred onto glass cover slips. Film patches were examined by means of optical microscopy prior to XRD measurements, in order to ensure that the crystal orientations are preserved during film transfer.

The X-ray powder diffraction pattern (data not shown) of calcite crystals growing underneath monolayers of **1** at π = 0.1 mN m^{-1} is dominated by (012) reflections centered at $2\theta = 23.07°$ (Cu-K_α) of the calcite crystal lattice,[21] while (104) reflections at $2\theta = 29.42°$, typical of calcite powder samples, are almost completely suppressed. This result indicates that the calcite (012) crystal planes are oriented parallel to the monolayer.

$CaCO_3$ crystals grown under monolayers of **1** show the

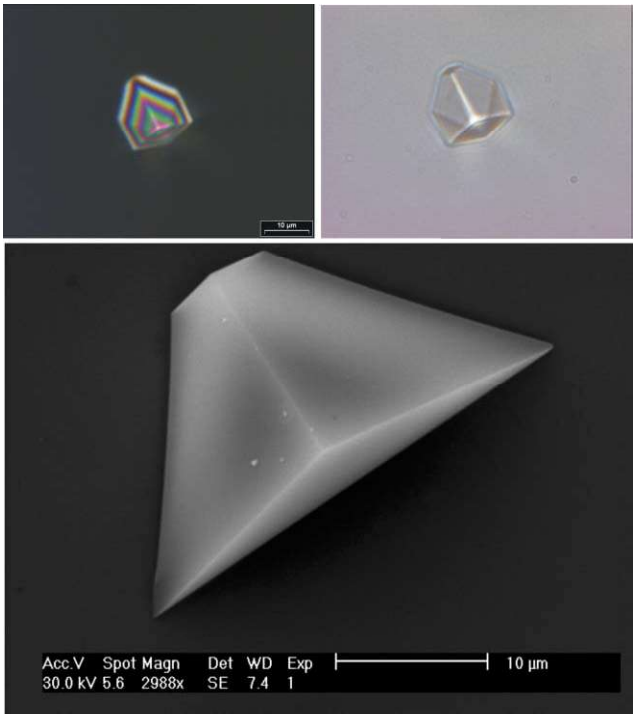

Fig. 9 Optical micrographs (crystals collected after 3 h) and scanning electron micrograph (crystals collected after 6 h) of (012) oriented calcite single crystals grown under a monolayer of **1** ($\pi = 0.1$ mN m^{-1}, $[Ca(HCO_3)_2]_{t=0} = 9$ mM).

characteristic shape of a (truncated) calcite {104} cleavage rhombohedron. The simple crystal morphology allows the determination of crystal orientation(s) from scanning electron micrographs (optical micrographs, respectively). A projection of rhombohedral faces onto the image plane of the micrograph yields characteristic interfacial angles, which can be assigned to the crystal's orientation. Thus, angle values determined from several micrographs such as those in Fig. 9 result in averages of about 152(2)°, 104(4)°, and 104(4)° which are characteristic of (012) oriented calcite rhombohedra.[5]

Matrix-templated growth of calcite single crystals showing a preferential (012) orientation has been reported for other self-assembled systems, including polymeric Langmuir–Schaefer films of 10,12-pentacosadiynoic acid,[3c] self-assembled monolayers of carboxylate-terminated alkanethiols supported on silver substrates,[4] as well as hydrogen-bonded molecular ribbons consisting of *N*,*N*′-dioctadecyltriazine-2,4,6-triamine and a cyanuric acid derivative.[3e] Much effort has been spent to correlate the periodicity of the calcite {012} cleavage plane with the putative monolayer structures. The polar {012} cleavage plane of calcite consists of separate layers of calcium and carbonate ions. Stabilization of this high-energy surface results from surface charge neutralization which most likely arises from coordination of anionic ligands, such as compound **1**, to the terminal (012) layer of Ca ions. However, the exact arrangement of ligands at the interface is hard to predict, considering the fact that the outward-bound Ca ions will become hydrated which should lead to considerable relaxation of their atomic positions.

It is hard to believe that the coincident growth of (012) oriented calcite crystals underneath monolayers of structurally dissimilar amphiphiles can be traced back to strict geometrical or even stereochemical matching of the two juxtaposed surfaces in all cases. We suggest that the epitaxy of calcite single crystals, which only occurs underneath monolayers of **1** at low surface pressure, is rather due to cooperative effects.[22] According to this, the surfactant monolayer should not be regarded as a rigid template. It is more likely that macroscopic materials properties such as average charge density or mean dipole moment of the templating monolayer determine the orientation of crystals. Our current investigations on oriented $CaCO_3$ crystal growth underneath monolayers of 5,11,17,23-tetrakis(1,1,3,3-tetramethylbutyl)-25,26,27,28-tetra(carboxymethoxy)calix[4]arene strongly support this hypothesis: in both cases, the (012) orientation of calcite crystals is prevailing.[6]

Summary

The crystal structures of *rccc*-5,11,17,23-tetracarboxy-4,6,10,12,16,18,22,24-octa-*O*-methyl-2,8,14,20-tetra(*n*-undecyl)-resorc[4]arene, **1**, as well as of its Ca salt, **2**, are analyzed in terms of the supramolecular packing arrangement of the constituting amphiphilic molecules. Both compounds form lamellar structures where the hydrophilic headgroups and the hydrophobic alkyl chains segregate into different layers. The packing arrangement of resorcarene moieties in both cases is governed by the sterically demanding macrocyclic headgroup. The *n*-undecyl chains of resorcarenes belonging to different layers are deeply interdigitated.

Monolayer experiments indicate that a similar packing arrangement can be predicted for monolayers of **1** spread at the air–water interface. The featureless Langmuir isotherms point to a liquid-condensed state of **1** throughout the investigated compression range.

$CaCO_3$ (calcite) single crystals grow underneath monolayers of **1** with highly uniform (012) orientation. This particular orientation is observed for a variety of structurally dissimilar monolayers, which leads us to conclude that macroscopic film properties such as average charge density or mean dipole moment have a decisive influence on templated calcite growth. Local supramolecular packing motifs are less important in those cases where calcite nucleation occurs at polar (highly charged) crystal faces.

Experimental

Synthesis

Melting points were determined on a Büchi B-540 apparatus and are uncorrected. IR spectra were recorded on a Perkin-Elmer 841 infrared spectrophotometer.

Synthesis of *rccc*-5,11,17,23-tetracarboxy-4,6,10,12,16,18,22,24-octa-*O*-methyl-2,8,14,20-tetra(*n*-undecyl)resorc[4]arene, **1**, will be described elsewhere.[20]

Calcium complex of 1: $[Ca(C_{84}H_{126}O_{16})(DMSO)_2(H_2O)_2]\cdot DMSO\cdot(H_2O)_4$, (2)

Compound **1** (34.8 mg, 0.025 mmol) was suspended in an aqueous solution of calcium acetate (8 mg, 0.05 mmol in 5 mL H_2O).

The suspension was treated ultrasonically and centrifuged. The remaining pellet was suspended with 5 mL water, treated ultrasonically and once again was centrifuged. The wet residue was dissolved in 10 mL dimethyl sulfoxide. Single crystals were grown by water vapor diffusion into the solution. Colourless plate-shaped crystals were obtained after 3 days.

Mp: 100 °C. IR (KBr): $\bar{\nu} = 3431, 2922, 2852, 1726, 1577, 1469, 1423, 1381, 1275, 1236, 1188, 1096, 1009, 951, 719$ cm^{-1}. Elemental analysis calcd. for $[C_{90}H_{156}O_{25}S_3Ca]$: C 61.82, H 8.93; found: C 62.95, H 9.99%.

Crystallography

X-Ray crystallographic data for *rccc*-5,11,17,23-tetracarboxy-4,6,10,12,16,18,22,24-octa-*O*-methyl-2,8,14,20-tetra(*n*-undecyl)-resorc[4]arene, 1. A single crystal of **1** was removed from the mother liquor and immediately cooled to 183 K on a Bruker AXS SMART diffractometer (three circle goniometer with 1 K

CCD detector, Mo-K_α radiation, graphite monochromator; hemisphere data collection in ω at 0.3° scan width in three runs with 606, 435 and 230 frames (Φ = 0, 88 and 180°) at a detector distance of 5 cm). A total of 76378 reflections ($1.12 < \theta < 22.52°$) were collected of which 24569 unique reflections (R(int) = 0.0425) were used. An empirical absorption correction using equivalent reflections was performed with the program SADABS.

Table 1 summarizes the crystallographic data and refinement parameters. The structure was solved by direct methods with the program SHELXS-97 and refined by full matrix least squares based on F^2 using SHELXL-97.[23] All hydrogen atoms were placed in calculated positions with the following parameters: $d(C_{ar}–H) = 0.95$ Å, $U(H) = 1.2\,U_{eq}(C)$; $d(C_{methylene}–H) = 0.99$ Å, $U(H) = 1.2\,U_{eq}(C)$; $d(C_{methyl}–H) = 0.98$ Å, $U(H) = 1.5\,U_{eq}(C)$; $d(O–H) = 0.84$ Å, $U(H) = 1.5\,U_{eq}(O)$.

X-Ray crystallographic data for $[Ca(C_{84}H_{126}O_{16})(DMSO)_2(H_2O)_2]\cdot DMSO\cdot(H_2O)_4$, 2. Thin colourless crystal plates of **2** were grown from water vapor diffusion into a DMSO solution of **2** at room temperature.

A single crystal of **2** was removed from the mother liquor and immediately cooled to 183 K on a Bruker AXS SMART diffractometer (three circle goniometer with 1 K CCD detector, Mo-K_α radiation, graphite monochromator; hemisphere data collection in ω at 0.3° scan width in four runs with 606, 500, 606 and 500 frames (Φ = 0, 88, 180 and 268°) at a detector distance of 5 cm). A total of 45705 reflections ($1.47 < \theta < 25.01°$) were collected of which 17813 unique reflections (R(int) = 0.0488) were used. An empirical absorption correction using equivalent reflections was performed with the program SADABS. Table 1 summarizes the crystallographic data and refinement parameters. The structure was solved by direct methods with the program SHELXS-97 and refined by full matrix least squares based on F^2 using SHELXL-97. All hydrogen atoms were placed in calculated positions (see above).

Monolayer experiments

Monolayer experiments were performed with a double-barrier NIMA trough using a compression speed of 15 $cm^2\,min^{-1}$. The surface pressure of the monolayers was measured using a Wilhelmy plate. The surfactant was spread using a chloroform solution (10 µl, 0.6 mg mL^{-1}). Compression was started after 10 min.

$CaCO_3$ crystal growth experiments

Solutions of calcium bicarbonate were prepared by bubbling carbon dioxide gas through a stirred aqueous (Millipore, resistance 18.2 MΩ cm) solution of $Ca(HCO_3)_2$ (9 mM) for a period of 2 h. Compressed films were formed by adding known amounts of surfactant to generate a liquid- or solid-like film at the air–water interface. Crystals were studied after several times either *in situ* by optical (polarization) microscopy (Olympus IX 70) or on cover slips laid on the film. The cover slips were also mounted on scanning electron microscope (SEM) specimen tubs. A Phillips XL30 ESEM operating at 30 keV was used. Bulk samples for X-ray diffraction (XRD) were obtained by collecting the crystals on cover slips laid on the film and removed horizontally. A Philips PW 1050/70 X-ray powder diffractometer was employed (2θ scans, Bragg–Brentano para-focussing geometry) using CuK_α radiation (λ = 1.54 Å).

Crystallographic indices are presented in three-index (*hkl*) notation, based on the hexagonal setting of the calcite unit cell ($R\bar{3}c$, a = 4.96 Å, c = 17.002 Å).

Acknowledgements

D. V. and M. F. thank the Deutsche Forschungsgemeinschaft (DFG) for financial support of their work (DFG grant Vo829/2-1). C. A.and J. M. are grateful to the DFG and the Fonds der Chemischen Industrie for financial support.

References

1 (*a*) H. A. Lowenstam and S. Weiner, *On Biomineralization*, Oxford University Press, Oxford, 1989; (*b*) A. P. Wheeler and C. S. Sikes, in *Biomineralization*, ed. S. Mann, VCH, Weinheim, 1989, pp. 95–131; (*c*) S. Weiner and L. Addadi, *J. Mater. Chem.*, 1997, **7**, 689.

2 S. Weiner and L. Addadi, in *Biomineralization*, ed. S. Mann, VCH, Weinheim, 1989, pp. 133–156.

3 (*a*) S. Mann, B. R. Heywood, S. Rajam and J. D. Birchall, *Nature*, 1988, **334**, 692; (*b*) S. Rajam, B. R. Heywood, J. B. A. Walker, S. Mann, R. J. Davey and J. D. Birchall, *J. Chem. Soc., Faraday Trans.*, 1991, **87**, 727; (*c*) A. Berman, D. J. Ahn, A. Lio, M. Salmeron, A. Reichert and D. Charych, *Science*, 1995, **269**, 515; (*d*) G. Xu, N. Yao, I. A. Aksay and J. T. Groves, *J. Am. Chem. Soc.*, 1998, **120**, 11977; (*e*) S. Champ, J. A. Dickinson, P. S. Fallon, B. R. Heywood and M. Mascal, *Angew. Chem., Int. Ed.*, 2000, **39**, 2716; (*f*) P. J. J. A. Buijnsters, J. J. J. M. Donners, S. J. Hill, B. R. Heywood, R. J. M. Nolte, B. Zwanenburg and N. A. J. M. Sommerdijk, *Langmuir*, 2001, **17**, 3623.

4 (*a*) J. Aizenberg, A. J. Black and G. M. Whitesides, *J. Am. Chem. Soc.*, 1999, **121**, 4500; (*b*) J. Küther, G. Nelles, R. Seshadri, M. Schaub, H. J. Butt and W. Tremel, *Chem. Eur. J.*, 1998, **4**, 1834.

5 D. D. Archibald, S. B. Qadri and B. P. Gaber, *Langmuir*, 1996, **12**, 538.

6 D. Volkmer, M. Fricke, S. Siegel and D. Vollhardt, in preparation.

7 (*a*) A. Bayer, *Ber. Dtsch. Chem. Ges.*, 1872, **5**, 25; (*b*) A. Bayer, *Ber. Dtsch. Chem. Ges.*, 1872, **5**, 280.

8 (*a*) H. Erdtman, S. Högberg, S. Abrahamsson and B. Nilsson, *Tetrahedron Lett.*, 1968, **14**, 1679; (*b*) B. Nilsson, *Acta Chem. Scand.*, 1968, **22**, 732.

9 L. M. Tunstad, J. A. Tucker, E. Dalcanale, J. Weiser, J. A. Byrant, J. C. Sherman, R. C. Helgeson, C. B. Knobler and D. J. Cram, *J. Org. Chem.*, 1989, **54**, 1305.

10 D. J. Cram, *Science*, 1983, **219**, 1177.

11 (*a*) R. Moran, S. Karbach and D. J. Cram, *J. Am. Chem. Soc.*, 1982, **104**, 5826; (*b*) D. J. Cram, S. Karbach, Y. H. Kim, L. Baczynskyj and G. W. Kalleymeyn, *J. Am. Chem. Soc.*, 1985, **107**, 2575; (*c*) D. J. Cram, S. Karbach, H. E. Kim, C. B. Knobler, E. F. Maverick, J. L. Ericson and R. C. Helgeson, *J. Am. Chem. Soc.*, 1988, **110**, 2229; (*d*) D. J. Cram, S. Karbach, Y. H. Kim, L. Baczynskyj, K. Marti, R. M. Sampson and G. W. Kalleymeyn, *J. Am. Chem. Soc.*, 1988, **110**, 2554.

12 Reviewed in: P. Timmerman, W. Verboom and D. N. Reinhoudt, *Tetrahedron*, 1996, **52**, 2663.

13 (*a*) H. Adams, F. Davis and C. J. M. Stirling, *Chem. Commun.*, 1994, 2527; (*b*) F. Davis and C. J. M. Stirling, *J. Am. Chem. Soc.*, 1995, **117**, 10385.

14 (*a*) L. R. MacGillivray and J. L. Atwood, *Nature*, 1997, **389**, 469; (*b*) L. R. MacGillivray and J. L. Atwood, *J. Am. Chem. Soc.*, 1997, **119**, 6931; (*c*) L. R. MacGillivray and J. L. Atwood, in *Crystal Engineering: From Molecules and Crystals to Materials*, NATO Science Series C: Mathematical and Physical Sciences, Vol. **538**, ed. D. Braga, F. Grepioni and A.G. Orpen, Kluwer, Dordrecht, 1999, pp. 407–419; (*d*) T. Gerkensmeier, W. Iwanek, C. Agena, R. Fröhlich, S. Kotila, C. Näther and J. Mattay, *Eur. J. Org. Chem.*, 1999, 2257; (*e*) T. Gerkensmeier, C. Agena, W. Iwanek, R. Fröhlich, S. Kotila, C. Näther and J. Mattay, *Z. Naturforsch. B Chem. Sci.*, 2001, **56**, 1063.

15 H. Adams, F. Davis and C. J. M. Stirling, *Chem. Commun.*, 1994, 2527.

16 HEFKUY: E. Benedetti, C. Pedone, R. Iacovino, B. Botta, G. Dellemonache, M. C. Derosa, M. Botta, F. Corelli, A. Tafi and A. Santini, *J. Chem. Res. S*, 1994, **12**, 476.

17 POBCUE: S. Zahn, K. Müller and G. Mann, *Z. Kristallogr.*, 1994, **209**, 470.

18 (*a*) V. A. Arsentiev and J. Leja, in *Colloid and Interface Science*, Vol. **5**, ed. M. Kerker, Academic Press, New York, 1976, pp. 251–270; (*b*) G. T. Barnes, in *Colloid Science*, Vol. **2**, ed. D.H. Everett, Chemical Society, London, 1975, pp. 173–190.

19 (*a*) D. E. Hibbs, M. B. Hursthouse, K. M. Abdul Malik, H. Adams, C. J. M. Stirling and F. Davis, *Acta Crystallogr., Sect. C*, 1998, **54**, 987;

(*b*) Davis, A. J. Lucke, K. A. Smith and C. J. M. Stirling, *Langmuir*, 1998, **14**, 4180.
20 D. Volkmer, M. Fricke, C. Agena and J. Mattay, in preparation.
21 Joint Committee on Powder Diffraction Standards – International Center for Diffraction Data, Swarthmore, PA, USA, 1986; File No. 24-27 (calcite).
22 M. J. Lochhead, S. R. Letellier and V. Vogel, *J. Phys. Chem. B*, 1997, **101**, 10821–10827.
23 SHELXS/L/H, SADABS from G.M. Sheldrick, University of Göttingen, 1997.